In situ analysis of the tribochemical films formed by SiC sliding against Mo in partial pressures of SO_2, O_2, and H_2S gases

I. L. Singer[a)]
Naval Research Laboratory, Code 6176, Washington, D.C. 20375

T. Le Mogne,[b)] C. Donnet,[c)] and J. M. Martin[d)]
Laboratoire de Tribologie et Dynamique des Systèmes, URA CNRS 855, Ecole Centrale de Lyon, 69131 Ecully Cedex, France

(Received 9 February 1995; accepted 21 October 1995)

X-ray photoelectron spectroscopy (XPS) and Auger electron spectroscopy (AES) were used to identify gas reaction layers and tribochemical films formed during reciprocating sliding tests in an ultrahigh vacuum (UHV) tribometer. Tests were performed on UHV cleaned SiC pins and Mo flats during or after exposure to SO_2, O_2, or H_2S gas at pressures around 40 Pa. XPS identified the gas reaction layers on Mo to be chemisorbed MoS_2 and/or MoO_2 phases less than 1 nm thick. AES of Mo wear tracks showed tribochemical films similar in composition to, but thicker than, the reaction layers. AES of SiC wear scars in all three gases indicated tribochemical films containing Si oxide and/or Si sulfide and possibly graphite. In addition, transfer films of Mo oxysulfide and Mo oxide were found in SO_2 and O_2 tests, respectively, but no transfer films were detected in H_2S tests. Thermochemical calculations of stable reaction products of the gas–solid reactions were in good agreement with the phases inferred from XPS and AES. An explanation for the agreement between thermochemical predictions and tribochemical results is given.

I. INTRODUCTION

The presence or absence of a surface film can determine the fate of counterface materials in sliding contact. If the counterface surfaces contain easily sheared films, then sliding will take place with low friction and virtually no counterface wear. In practical machinery, surfaces often develop shearable films during exposure oxygen and various contaminants in air. Unfortunately, these ''air-formed'' films are not very durable, nor can they sustain low friction. Other gases, however, have been shown to sustain low friction and protect solid surfaces from wear: H_2S on Mo,[1] I_2 on Ti and Cl_2 on Cr,[2] TCP on steel,[3] and hydrocarbons on ceramics.[4] The protection is not due to gases, but to the ''tribochemical'' films formed when surfaces are rubbed against each other in the presence of the gases. These tribochemical films have been identified by *ex situ* analytical techniques for sliding in air[5–7] and in selected gases at high temperatures.[3,4] Unfortunately, the mechanics and chemistry of tribochemical film formation are not well understood. Well-controlled *in situ* experiments, as performed in the present study, are required to investigate how tribochemical films are generated; results of such studies will enable tribologists to chose the correct gaseous environments for specific tribomaterials, thereby providing low friction and wear-free surfaces, with tremendous safety and cost benefits.

Buckley[8] and his colleagues at NASA Lewis Space Center in the 1970s pioneered the use of *in situ* tribometry and surface spectroscopy in an ultrahigh vacuum (UHV) chamber. In studies of solid–solid reactions[9] and gas–solid interactions[10–12] at gas pressures at or below 1 mPa, they demonstrated that gas reaction layers could decrease (or increase!) friction coefficients. However, the layers wore away after one or two passes, and the friction coefficient returned to its UHV value.[9,12] More recently, Pope *et al.*,[13,14] DeKoven *et al.*,[15,16] and Le Mogne *et al.*[17,18] have used multianalytical UHV tribometers to examine the friction behavior of materials exposed to reactive gases at pressure above 1 Pa. In all cases, low friction sliding could be sustained and distinct tribochemical reaction products detected on worn surfaces.

We have used a similar approach to investigate the lubrication of SiC sliding against Mo in SO_2, O_2, and H_2S gases at pressures up to 40 Pa. SiC was chosen as the pin because of its hardness and its ease of cleaning in UHV. Mo was selected because its reaction with H_2S is expected to produce MoS_2,[1] the lowest friction film yet discovered;[19] friction coefficients of MoS_2 typically range from $\geqslant 0.01$ in dry air to as low as 0.001 in vacuum, depending on film preparation conditions.[20] The two oxygen-containing gases were chosen because they are intimately related to the chemical degradation of MoS_2 in (dry) air: O_2 is responsible for the most prominent tribochemical reaction products in (dry) air,[5] and SO_2 is a gaseous reaction product of oxidized MoS_2. The results of the friction tests, reported earlier,[21] revealed three orders of magnitude differences in the steady state friction coefficients, depending on gas type and pressure at which the tests were run. Friction coefficients run in SO_2 and O_2 at pressures around 40 Pa were about $\mu \geqslant 0.1$; in H_2S, the friction was more than an order of magnitude lower, μ

a)Electronic mail: singer@ccf.nrl.navy.mil
b)Electronic mail: lemogne@cc.ec-lyon.fr
c)Electronic mail: donnet@cc.ec-lyon.fr
d)Electronic mail: martinj@cc.ec-lyon.fr

Report Documentation Page

Form Approved
OMB No. 0704-0188

1. REPORT DATE	2. REPORT TYPE	3. DATES COVERED
1996		**00-00-1996 to 00-00-1996**

4. TITLE AND SUBTITLE	5a. CONTRACT NUMBER
In situ analysis of the tribochemical films formed by SiC sliding against Mo in partial pressures of SO2, O2, and H2S gases	5b. GRANT NUMBER
	5c. PROGRAM ELEMENT NUMBER
6. AUTHOR(S)	5d. PROJECT NUMBER
	5e. TASK NUMBER
	5f. WORK UNIT NUMBER
7. PERFORMING ORGANIZATION NAME(S) AND ADDRESS(ES) **Naval Research Laboratory,Code 6176,4555 Overlook Avenue, SW,Washington,DC,20375**	8. PERFORMING ORGANIZATION REPORT NUMBER
9. SPONSORING/MONITORING AGENCY NAME(S) AND ADDRESS(ES)	10. SPONSOR/MONITOR'S ACRONYM(S)
	11. SPONSOR/MONITOR'S REPORT NUMBER(S)

12. DISTRIBUTION/AVAILABILITY STATEMENT
Approved for public release; distribution unlimited

13. SUPPLEMENTARY NOTES

14. ABSTRACT

15. SUBJECT TERMS

16. SECURITY CLASSIFICATION OF:			17. LIMITATION OF ABSTRACT	18. NUMBER OF PAGES	19a. NAME OF RESPONSIBLE PERSON
a. REPORT **unclassified**	b. ABSTRACT **unclassified**	c. THIS PAGE **unclassified**		**8**	

<0.01. In contrast, friction coefficients for a pin and flat that had been exposed to H_2S at pressures up to 40 Pa for several hours but run under high vacuum conditions, about 3×10^{-6} Pa, were about $\mu=1$ after one pass, indicating that surfaces pre-exposed to H_2S were unable to sustain low friction. A detailed presentation and discussion of the friction and wear behavior observed in these tests are presented elsewhere.[21]

The purpose of this article is to identify the surface films that might be responsible for these large differences in friction behavior. X-ray photoelectron spectroscopy (XPS) and Auger electron spectroscopy (AES) were used to characterize both the gas exposed and the worn surfaces. Compositions and thickness of films generated by gas–solid reactions (gas reaction layers) and by sliding (tribochemical films) were determined and compared to those of films identified by other surface analytical techniques and phases predicted by thermochemistry.

II. EXPERIMENT

A. Friction and surface analysis apparatus

Wear tests and surface analysis were carried out *in situ* in a loadlocked, multitechnique UHV chamber described in detail in previous papers.[17,18] The tribometer consisted of a pin loaded against a flat; both pin and flat could be repositioned *in situ* to perform from four to eight tests without removing either sample from the UHV chamber. The chamber could be backfilled with gas and its pressure regulated between 0.1 and 1000 Pa using a capacitance manometer (MKS baratron) in feedback with a mass flow meter. Surfaces were analyzed by XPS and AES using a VG hemispherical analyzer. XPS was acquired over a wide area (about 1 cm^2) with nonmonochromatized Mg $K\alpha$ x rays. AES was taken with a 5 keV electron beam whose submicrometer spot size was broadened to between 5 and 20 μm by rastering. Sputter cleaning was performed with 5 keV Ar ions.

B. Sample preparation and friction test procedures

A rod of α-SiC was ground on one end to form a hemispherical pin of radius 1.8 mm. The pin and a 1-mm-thick polycrystalline Mo flat were polished with successively finer pastes of 6, 3, and 1 μm diamond. After cleaning with solvent, both the SiC and the Mo were inserted through a loadlocked chamber into the UHV chamber. The substrates were first cleaned by radiative heating to about 800 °C, then by Ar ion sputtering for 15–30 minutes. XPS and AES were taken to establish the cleanliness of the two surfaces.

Wear tests were run at pressures between 4 and 40 Pa. The chamber was filled with one of the three test gases, SO_2, O_2, or H_2S, the substrates loaded into contact, then sliding tests were run for 60 cycles. The load was 0.5 N, equivalent to an initial mean contact pressure of 0.7 GPa, well below the hardness (2.9 GPa) of the softer Mo counterface. The stroke distance was 3 mm, and the speed was 0.5 mm/s.

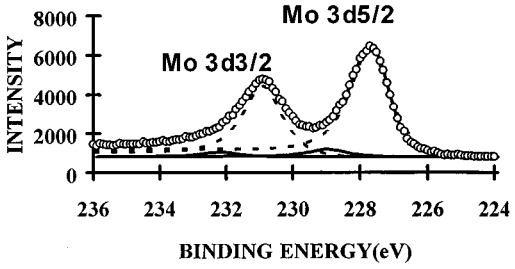

FIG. 1. XPS of Mo 3*d* 5/2 and Mo 3*d* 3/2 on a Mo surface exposed to H_2S for 2 hours at pressures from 4 to 40 Pa. Deconvoluted peaks are shown as solid and dashed lines; measured spectrum is given by open circles.

C. Surface analysis procedures

XPS analysis was performed on Mo before and after sputter cleaning and after each gas exposure. Both survey and high energy resolution XPS spectra were acquired. The high resolution spectra of Mo 3*d*, S 2*p*, and O 1*s* were taken with a 50 eV pass energy. The peaks were deconvoluted and fitted using the Sherwood model (Gaussian–Lorentzian/Shirley background). Binding energies (BE) were referenced to the Au 4*f* 7/2 peak at 84.0 eV; BE uncertainty was $\pm$ 0.2 eV. Phases associated with these peaks were identified by the binding energy of standards reported in the literature.[22,23] AES analysis was performed on Mo and SiC before sputter cleaning and after each gas exposure. Secondary electron images were used to locate wear tracks on Mo and wear scars on SiC. Spectra were acquired in the *N(E)* mode, then differentiated for peak-height analysis.

III. RESULTS

A. XPS analysis

XPS surveys (not shown) indicated that sputter cleaned and gas exposed surfaces had significantly lower C and O intensities than the polished surface, but nonetheless had trace quantities of C and O. Figure 1 shows high-resolution XPS spectra of Mo 3*d* 5/2 and Mo 3*d* 3/2 of the H_2S-exposed surface; both raw data and deconvoluted peaks are shown. Two chemical states of Mo can be seen; in the 3*d* 5/2 spectra, they are a large 227.7 eV peak and a smaller, higher binding energy peak at 229.2 eV. Peak-fitted binding energies and areal intensities for Mo 3*d* 5/2, S 2*p*, and O 1*s* on the polished and four vacuum-prepared surfaces are presented in Table I.

B. AES analysis

AES, like XPS, found low levels of contaminants O and C (and sometimes S) on sputter-cleaned surfaces. Since similar levels were seen after gas exposure as well, they must represent ''background'' levels of surface contamination. AES spectra were taken inside and outside the worn areas (wear tracks) of the Mo flat but only inside wear scars on the SiC pin.

TABLE I. XPS binding energies (BE) and areal intensities (I) of the main peaks on an Mo surface exposed to gases at pressures from 4 to 40 Pa. Data on polished and sputtered Mo are given for reference.

Peaks		Surface treatment/gas exposure				
		Polished	Sputtered	SO_2	O_2	H_2S
Mo 3*d* 5/2	BE (eV)	227.6	227.7	227.9	227.9	227.7
	I (counts eV/s)	4786	14493	11909	10361	9212
	BE (eV)	229.4	⋯	230.0	229.4	229.2
	I(counts eV/s)	1931	⋯	1304	1890	537
	BE (eV)	232.6	⋯	⋯	⋯	⋯
	I(counts eV/s)	1677	⋯	⋯	⋯	⋯
O 1*s*	BE (eV)	529.8	⋯	529.7	529.7	⋯
	I(counts eV/s)	4970	⋯	1367	2018	⋯
	BE (eV)	531.8	⋯	530.8	531.2	⋯
	I(counts eV/s)	4573	⋯	690	480	⋯
S 2*p*	BE (eV)	⋯	⋯	161.5	⋯	161.5
	I(count eV/s)	⋯	⋯	447	⋯	700

1. Tracks on Mo

Representative spectra taken inside and outside tracks on Mo are shown in Fig. 2. The spectra indicate similar compositions in both locations. However, peak-to-peak intensities of the S(KLL) and O(KLL) spectra were larger inside the track than outside the track. The opposite was found for the C(KLL) intensity, which was larger outside than inside, suggesting that C was an adsorbed contaminant that was partially wiped off during the friction tests.

In SO_2 tests, S/Mo and O/Mo ratios in the tracks were about twice that of ratios outside the track. The peak near 130 eV could not be identified with certainty: it might be the Mo($M_{4,5}N_{2,3}N_{2,3}$) feature, but this should be considerably smaller than the 180 eV peak, even in the oxide state;[24] or it might be a surface sulfate peak,[25] although no Mo sulfate exists in the bulk. Tracks in O_2 tests showed mainly oxidized Mo, with the O/Mo ratio in the track twice that outside of track. S was also detected, but the S/Mo was about the same inside and outside, indicating that S was a background contaminant. Finally, tracks in H_2S tests had a S/Mo ratio about 1.5 times that of unworn areas and no O.

2. Scars on SiC

Spectra taken on clean SiC and in wear scars are shown in Fig. 3; note that the spectra shifted about +30 eV above expected energies due to charging. The cleaned pin showed Si(LVV) and C(KLL) characteristic of SiC and a small O(KLL) intensity. Spectra of scars in all three gases showed some S and/or O as well as changes in the line shapes of Si(LVV) and C(KLL) spectra.

The scar formed in SO_2 showed Mo as well as S and O, and the S/Mo ratio (=4.5) was the same as found in the track on Mo. Apparently, Mo oxide and Mo sulfide transferred from the Mo wear track to the SiC scar. The C/Si ratio in the scar was only 60% of the ratio on clean SiC. Moreover, the line shapes of both Si(LVV) and C(KLL) differed from that of SiC: the C(KLL) has a low-energy feature that makes it appear graphite-like,[26,27] and the Si(LVV) has a low energy peak that could be an oxide or a sulfide. These features suggest that some SiC converted to graphite plus Si oxide or Si sulfide. The scar formed in O_2 showed mainly Mo and O with a very distorted Si(KLL) line, suggesting Si oxide and very little SiC. Here again the O/Mo ratios were nearly the

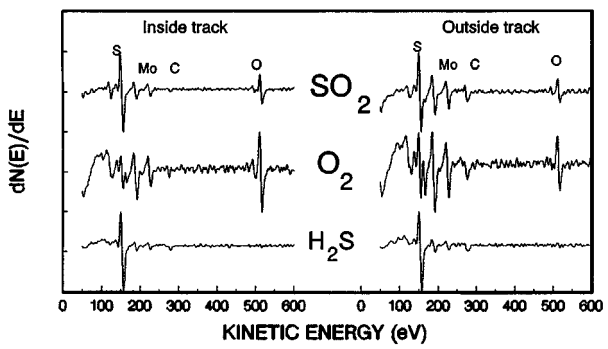

FIG. 2. *In situ* AES spectra taken inside and outside tracks on Mo.

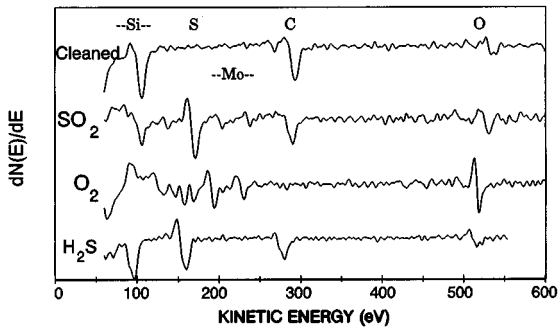

FIG. 3. *In situ* AES spectra taken of a sputter-cleaned area and wear scars on the SiC pin.

TABLE II. Phase and thickness of surface layers on gas-exposed Mo surfaces measured by XPS.

Surface treatment	Polished	SO_2	O_2	H_2S
Phase	MoO_3 on MoO_2	MoO_2, MoS_2	MoO_2	MoS_2
Thickness (nm)	1.0 + 1.4	0.5	0.7	0.3

same as on the Mo track, suggesting that Mo oxide films transferred to SiC.

Finally, AES spectra of scars formed in H_2S consistently showed a strong S signal but little or no Mo, indicating that MoS_2 films *did not transfer* to SiC during sliding. The C(*KLL*) line shape looked like a mixture of graphite and SiC, while the low energy shoulder on the Si(*KLL*) line might be that of Si sulphide since it is not shifted enough to be Si oxide.

IV. DISCUSSION

A. Gas reaction layers

The compositions of gas reaction layers can be inferred from the binding energies in Table I. The Mo 3*d* 5/2 spectrum of the sputter-cleaned surface showed only one peak, the Mo^0 of metallic Mo. The three gas-exposed surfaces had only two peaks: the larger peak is metallic Mo and the smaller peak is a Mo^{4+} state. The Mo^{4+} peaks correspond to MoO_2 and MoS_2 in SO_2 gas, MoO_2 in O_2 gas, and MoS_2 in H_2S gas. The polished surface had three Mo 3*d* 5/2 peaks, corresponding to metallic, MoO_2, and MoO_3 (Mo^{6+}) phases. The single S 2*p* peak from SO_2- and H_2S-exposed Mo is that obtained with MoS_2. The two O 1*s* peaks in polished, SO_2-exposed and O_2-exposed Mo could be from MoO_2, a suboxide,[28] or OH^-; some OH^- adsorption is likely after pumpdown to UHV since H_2O was the major background gas. We do not concern ourselves hereafter with the O 1*s* peaks. Table II summarizes the phases of the gas reaction layers on four of the five samples: it shows that the gas–Mo reaction layers were chemisorbed phases of MoO_2 or MoS_2 or a mixture of the two.

Thicknesses of the gas reaction layers were calculated from the ratio of areal intensities of the Mo 3*d* 5/2 spectra in Table I.[29,30] Equations used to calculate thicknesses, t, of up to two layers on a metal are derived in the Appendix. Table II lists the calculated thicknesses for the gas reaction and polished layers. All three gas reaction layers were less than 1 nm thick, considerably thinner than the 2.4 nm oxide layer on polished Mo.

The compositions and thickness of gas reaction layers on polycrystalline Mo (Table II) may be compared with more detailed studies of gas reaction layers on single crystal Mo. According to the literature, at room temperature, O_2 forms a disordered, chemisorbed film, about 2 monolayers thick, on Mo(100) surfaces.[31] The film does not nucleate to a recognizable oxide phase [by low-energy electron diffraction (LEED) and Raman] until temperatures above 700 K[31] and film thickness above 0.6 nm.[32] Therefore, it is likely that the MoO_2 gas reaction layer on polycrystalline Mo, estimated here to be 0.7 nm thick (Table II), is only a chemisorbed film.

Similarly, sulfur chemisorbs onto single crystals of Mo at room temperature, but does not develop a basal-oriented MoS_2 structure at these pressures, ≈40 Pa, until high temperatures (at least 500 °C).[33] At room temperature, H_2S rapidly dissociates on Mo, saturating the surface at exposures less than 4 langmuir and forming a weakly ordered S layer (according to LEED).[34] This layer saturates at only one-third of a monolayer; growth to higher coverage with H_2S is impeded by chemisorbed H and S atoms, which interfere with the dissociative adsorption of H_2S on Mo.[35] (Coverage up to two-thirds monolayer thick is also possible if the dissociated H_2 can be driven off.) Recent quantitative LEED studies on Mo(100) indicate that, at high coverage, S bonds to (and distorts) two underlying Mo layers, which themselves sit 0.32 nm above the bulk Mo layers.[36] This value is in agreement with that of the MoS_2 reaction layer on polycrystalline Mo, found in Table II. We surmise, therefore, that the gas reaction layers formed on the Mo substrates were thin, chemisorbed films and not crystalline oxide or sulfide films.

Gas reaction films on SiC were not analyzed here. However, several studies of SiC exposed to O_2 at room temperature have been reported. Polycrystalline SiC exposed to O_2 at pressures of 50 Pa had only a physisorbed layer of oxygen.[17] Single crystal SiC exposed at 50 Pa did not show the expected highly exothermic reaction $O_2 + SiC \leftrightarrow SiO_2 + C$; instead, oxygen was weakly bound (as Si–O–Si) to the surface.[37] Therefore, under present conditions of room temperature and 40 Pa, oxidation of the surface of the SiC pin is not expected.

B. Tribochemical films

Compositions of tribochemical films were inferred from AES line shapes and the peak height ratios. On Mo, films in the track had the same elemental compositions as those outside the track (i.e., gas reaction films), but higher intensities of the chemisorbed element (O, O+S or S). We speculate that tribochemical films had the same phases but were thicker than the gas reaction films. In H_2S, we suggest that the increased S intensity arose from an increased in H_2S chemisorption and that the limitation imposed on the S coverage due to chemisorbed H (Ref. 35) was lifted by the rubbing process. In fact, the S/Mo ratio for the film was the same as that of an MoS_2 layer measured for ultralow friction MoS_2 films.[38] Rubbing could also have allowed more O to chemisorb on the Mo wear track by increasing the number of defect sites. It is not clear, however, which oxide—MoO_2 or MoO_3 or one of the substoichiometric MoO_x ($2 < x < 3$) compounds—formed, although MoO_2 is the first to crystallize from the chemisorbed state with increasing thermal activity.[31,32] We therefore designate the oxide to be MoO_x. In SO_2, mixtures of MoS_2 and MoO_x would be expected.

On the SiC wear scar, three possible tribochemical films have been inferred from Auger analysis: Si oxide (SiO_y, $y=1$ or 2), Si sulfide (SiS_z, $z=1$ or 2), and graphite (C). The

TABLE III. Tribochemical and transfer films found on Mo and SiC after sliding in gases at pressures from 4 to 40 Pa. Phases were inferred from Auger data. ($2 \leqslant x \leqslant 3$; y, $z = 1$ or 2.)

	Solid			
	Mo		SiC	
Gas	Tribofilm	Transfer	Tribofilm	Transfer
SO_2	MoO_x/MoS_2	None	SiO_y/SiS_z, C	MoO_x/MoS_2
O_2	MoO_x	None	SiO_y	MoO_x
H_2S	MoS_2	None	SiS_z, C	None

Si oxide and graphite phases were clearly tribochemical films since, as mentioned earlier, the reaction $O_2+SiC \rightarrow SiO_2+C$ does not take place at room temperature. In addition, films having roughly the same compositions as the tribochemical films on Mo also collected on the SiC scar run in SO_2 and O_2. These films were transferred during sliding from the Mo track surface to the SiC pin. Table III summarizes the compositions of tribochemical and transfer films generated during sliding.

C. Tribochemistry and thermochemistry

Currently there are no accepted models for tribochemical reactions. One school of thought is that tribochemical processes are nonequilibrium and therefore tribochemical films are nonequilibrium products of chemical reactions.[39] A second school contends that rubbing stimulates reaction by mechanical deformations at the atomic and mesoscopic scales, thereby speeding reaction rates at low temperatures.[40] Singer[7] has built upon the latter hypothesis and suggested that, when thin layers wear slowly in reactive gases, the defects generated will enhance the reaction rate sufficiently to form thermochemically stable products. In the present case of nominally clean surfaces exposed to reactive gases, we speculate that the defects formed by the strains induced during sliding provide a driving force for phase formation on worn surfaces in the same way that high temperatures do on pristine surfaces. If this hypothesis is true, then the tribochemical films should have the same compositions as those predicted by thermochemistry.

Simple thermochemical calculations have been performed for two and three element gas–solid reactions using methods described earlier.[5–7] Selected results for gas reactions with Mo and SiC are presented in the two ternary diagrams shown in Fig. 4. The diagrams were computed using Gibbs free energy data valid at $T=298$ K and $p=0.1$ MPa.[41] The tie lines were obtained by writing balanced equations for the reactants and products and determining the side that had the lower free energy. The stable products can be seen at the vertices of each of the triangles through which the reaction line passes. We see, for example, that MoO_3 cannot be a reaction product in the ternary reaction of $Mo+SO_2$, but it is a reaction product of the binary reaction $Mo+O_2$.[42] We also see that C and SiO_2 are reaction products of O_2 with SiC but that SiO isn't.

Although these simple calculations are instructive, more sophisticated computational techniques are needed to establish equilibrium phases at arbitrary gas pressures and for reactions of four or more elements. To this end, a commercial program, F*A*C*T,[43] was used to perform more detailed thermochemical calculations. Reaction products were determined for six pairs of reactants, one pair for each of the three gases with Mo and with SiC. For example, the reaction products from mixtures of SiC with SO_2 were obtained by inputing $\langle A \rangle$ SiC+$\langle 1-A \rangle$ SO_2 for values $0 \leqslant A \leqslant 1$. Free energies were calculated at $T=298$ K and $p=10$ Pa for all possible reactants in each system. Thermodynamic data in the F*A*C*T database were used; the database provided upwards of 80 gases, liquids and solids in each of the ternary or quaternary systems. Gibbs phase rule, we remind, requires that the number of stable products for a given concentration of reactants at constant temperature and pressure be no more than the number of elements; therefore, at any particular concentration, one gets only two stable products from the binary reaction Mo plus O_2, three from the ternary reactions of SO_2 or H_2S with Mo and O_2 with SiC, but four from the quaternary reactions of SO_2 or H_2S with SiC.

Table IV lists a complete set of stable reaction products for the six gas–solid reactions studied, in order of solid-rich to gas-rich reaction products; we focus here on the solid phases. In the Mo–gas systems, the predictions—mixed MoO_2 and MoS_2 in SO_2 gas, MoO_2 or MoO_3 in O_2, and MoS_2 in H_2S—are consistent with the phases inferred for the tribochemical films in Table III as well as the gas–reaction films in Table II. In the SiC–SO_2 system, products include SiO_2, SiS, and SiS_2, C (graphite) and solid S; in the

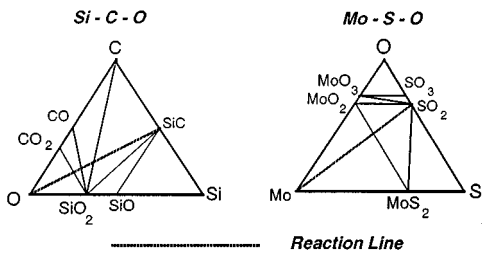

FIG. 4. Ternary diagrams calculated for the Mo–S–O and Si–C–O systems at standard temperature (298 K) and 1 atm (0.1 MPa) pressure.

TABLE IV. Equilibrium phases of solid–liquid–gas reactions at $T=298$ K and $p=10$ Pa, calculated using F*A*C*T, a SOLGASMIX program (Ref. 43). (s): solid; (g): gas.

	Solid	
Gas	Mo	SiC
SO_2	Mo(s), MoS_2(s), MoO_2(s) MoS_2(s), MoO_2(s), SO_2(g)	SiC(s), C(s), SiO_2(s), SiS(s) C(s), SiO_2(s), SiS(s), SiS_2(s) C(s), SiO_2(s), S(s), CO_2(g) SiO_2(s), S(s), CO_2(g), SO_2(g)
O_2	Mo(s), MoO_2(s) MoO_2(s), MoO_3(s) MoO_3(s), O_2(g)	SiC(s), SiO_2(s), C(s) C(s), SiO_2(s), CO(g) SiO_2(s), CO(g), CO_2(g) SiO_2(s), CO_2(g), O_2(g)
H_2S	Mo(s), H_2(g), MoS_2(s) H_2(g), MoS_2(s), H_2S(g)	SiC(s), SiS(s), C(s), CH_4(g) SiS(s), C(s), CH_4(g), SiS_2(s) C(s), CH_4(g), SiS_2(s), H_2S(g)

SiC–O_2 system, SiO_2 and graphite are predicted; and in the SiC–H_2S system, SiS, SiS_2, and graphite are predicted. These results are also consistent with the phases inferred from the AES spectra in Table III. However, the present spectra were too noisy to make exact identifications; we shall attempt to clarify these phases in a later experiment. The calculations, nonetheless, support the hypothesis that tribochemical films (and gas reaction films) have the same compositions as films formed in thermochemical equilibrium.

V. SUMMARY AND CONCLUSIONS

Surface films present before and after sliding of SiC against Mo in SO_2, O_2, or H_2S, at pressures between 4 and 40 Pa, have been identified. Gas reaction layers on Mo were shown to be thin (<0.7 nm) chemisorbed films of Mo^{4+} species, MoO_2, and/or MoS_2. The tribochemical films generated on Mo in the three gases had the same elemental compositions as the corresponding gas reaction layers but appeared to be thicker. Tribochemical films on SiC consisted of a Si oxide and/or Si sulfide plus C. Moreover, the wear scars on SiC run in SO_2 and O_2 runs contained Mo oxysulfide and Mo oxide transfer films, whereas those run in H_2S had no transfer film. Compositions of both gas reaction layers and tribochemical films were in good agreement with gas–solid reaction products calculated by equilibrium thermochemistry.

ACKNOWLEDGEMENTS

One of the authors (I.L.S.) wishes to acknowledge the Naval Research Laboratory for supporting a sabbatical stay at Ecole Centrale de Lyon during FY93 and to thank M. Salmeron and A. Gellman for helpful discussions on gas reaction films and K. Wahl for critical comments on the manuscript.

APPENDIX: THICKNESS OF TWO COMPOUND OVERLAYERS ON Mo FROM XPS DATA

	Compound	IMFP	Thickness
MoO_3	C	λ_C	t_C
MoO_2	B	λ_B	t_B
Mo	A	λ_A	

The thicknesses, t_C and t_B, of two compound overlayers, C and B, on metal A, such as MoO_3 and MoO_2 layers on Mo illustrated in the two-layer model above, can be calculated as follows:

$$I_m^A = I_\infty^A[\exp(-t_B/\lambda_B \sin\theta)][\exp(-t_C/\lambda_C \sin\theta)], \quad (1)$$

$$I_m^B = I_\infty^B[1-\exp(-t_B/\lambda_B \sin\theta)][\exp(-t_C/\lambda_C \sin\theta)], \quad (2)$$

$$I_m^C = I_\infty^C[1-\exp(-t_C/\lambda_C \sin\theta)], \quad (3)$$

where I_m^X=measured Mo 3*d* peak intensity from layer *X*, I_∞^X=Mo 3*d* peak intensity from an infinitely thick layer of *X*, λ_X = inelastic mean free path (IMFP) of the Mo 3*d* electron in *X*, and θ=the angle between detector and surface (75 °C).

Thickness t_B is found by taking the ratio of Eqs. (1) and (2):

$$I_m^A I_\infty^B/(I_m^B I_\infty^A)$$

$$=\exp(-t_B/\lambda_B \sin\theta)/[1-\exp(-t_B/\lambda_B \sin\theta)]. \quad (4)$$

Equation (4) can be rewritten as

$$I_\infty^B/I_\infty^A = N^B\lambda_B/N^A\lambda_A, \quad (5)$$

TABLE AI. Chemical properties, IMFP, and layer thickness, t, MoO_3 and MoO_2 on Mo. Data for MoS_2 and MoOS (average of MoS_2 and MoO_2), are given for reference.

Compound	MW (kg/mole)	ρ (kg/m^3)	n (atoms/ molecules)	a (nm)	IMFP (nm)	Area (count eV/s)	t (nm)
Mo	0.0959	10200	1	0.25	1.6	4786	⋯
MoO_2	0.1279	6470	3	0.22	2.4	1931	1.4
MoO_3	0.1439	4690	4	0.23	2.6	1677	1.0
MoS_2	0.1601	4800	3	0.26	3.1	⋯	⋯
MoOS	0.1439	5635	3	0.24	2.7	⋯	⋯

where N^X is the atomic density of the Mo 3d electron in compound X. Rearranging Eqs. (4) and (5) to solve for t_B gives

$$t_B = \lambda_B \sin\theta \ln[(N^A\lambda_A I_m^B)/(N^B\lambda_B I_m^A)+1]. \quad (6)$$

Equation (6) is the solution for the thickness of a single thin layer, B, on A. Thickness t_C is found by taking the ratio of Eqs. (2) and (3):

$$I_m^B I_\infty^C/(I_m^C I_\infty^B) = 1-\exp(-t_B/\lambda_B \sin\theta)/[\exp(t_C/\lambda_C \sin\theta)-1]. \quad (7)$$

and, by Eq. (5),

$$N^C\lambda_C I_m^B/N^B\lambda_B I_m^C = 1-\exp(-t_B/\lambda_B \sin\theta)/[\exp(t_C/\lambda_C \sin\theta)-1] \quad (8)$$

gives

$$t_C = \lambda_C \sin\theta \ln\{[N^B\lambda_B I_m^C)/(N^C\lambda_C I_m^B)] \times[1-\exp(-t_B/\lambda_B \sin\theta)]+1\}. \quad (9)$$

Equation (9) is the solution for the thickness of a second thin layer, C, on top of B on A.

The IMFPs for the Mo and MoX compounds can be calculated as[30]

$$\lambda_{Mo} = a[538E^{-2}+0.41(aE)^{0.5}],$$

$$\lambda_{MoX} = a[2170E^{-2}+0.72(aE)^{0.5}],$$

where E=kinetic energy=1024 eV and a=thickness of a monolayer (in nm). The thickness of a monolayer may be estimated as the 1/3 power of the atomic volume of the compound:

$$a^3 = \mathrm{MW}/(\rho n N_A)\times 10^{27},$$

where MW is molecular weight (in kg/mole), ρ is the density (in kg/m^3), n is the number of atoms in a molecule and N_A is Avogadro's number=6.02×10^{23} (in molecules/mole).

In Table AI, monolayer thickness, IMFP, and thickness of the MoO_2 and MoO_3 layers on polished Mo are calculated from area data taken from Table I.

Paper presented at the 41st National Symposium of the American Vacuum Society, Denver, CO, 24–28 October 1994.

[1]F. P. Bowden and D. Tabor, *The Friction and Lubrication of Solids* (Clarendon, Oxford, 1964), Part 2, p. 210.
[2]G. Rowe, Wear **3**, 247 (1960).
[3]E. E. Graham and E. E. Klaus, ASLE Trans. **29**, 229 (1986); E. E. Graham, A. Nesarikar, N. Forster, and G. Givan, Lubr. Eng. **49**, 713 (1993).
[4]J. L. Lauer, T. A. Blanchet, B. L. Vlcek and B. Sargent, Surf. Coat. Technol. **62**, 399 (1993); J. L. Lauer, B. L. Vlcek and B. Sargent, Wear **162**, 498 (1993).
[5]S. Fayeulle, I. L. Singer and P. D. Ehni, in *Mechanics of Coatings, Tribology*, Series 17, edited by D. Dowson, C. M. Taylor, and M. Godet (Elsevier, Amsterdam, 1990), p. 129.
[6]I. L. Singer, S. Fayeulle, and P. D. Ehni, Wear **149**, 375 (1991).
[7]I. L. Singer, Surf. Coat. Technol. 49, 474 (1991).
[8]D. H. Buckley, *Surface Effects in Adhesion, Friction, Wear and Lubrication* (Elsevier, Amsterdam, 1981), Chap. 6.
[9]K. Miyoshi and D. H. Buckley, ASLE Trans. **22**, 245 (1979).
[10]D. R. Wheeler, J. Appl. Phys. **47**, 1123 (1976).
[11]S. V. Pepper, J. Appl. Phys. **47**, 801 (1976); **50**, 8062 (1979).
[12]S. V. Pepper, J. Appl. Phys. **47**, 2579 (1976).
[13]L. E. Pope and D. E. Peebles, Tribology Trans. **31**, 202 (1988); L. E. Pope and D. E. Peebles, IEEE Trans. Components, Hybrids, Manuf. Technol. **CHMT-11**, 124 (1988).
[14]D. E. Peebles, L. E. Pope, and D. M. Follstaedt in *Surface Diagnostics in Tribology*, edited by K. Miyoshi and Y. W. Chung (World Scientific, Singapore, 1993), pp. 205–270.
[15]B. M. DeKoven and G. Meyers, J. Vac. Sci. Technol. A **9**, 2570 (1991).
[16]B. M. DeKoven, in Ref. 14, pp. 299–342.
[17]J. M. Martin and T. Le Mogne, Surf. Coat. Technol. **49**, 427 (1991).
[18]T. Le Mogne, C. Donnet, J. M. Martin, and A. Tonck, J. Vac. Sci. Technol. A **12**, 1998 (1994).
[19]I. L. Singer, in *New Materials Approaches to Tribology: Theory and Applications*, edited by L. Pope, L. Fehrenbacher, and W. Winer, Proceedings of the Materials Research Socieity Symposium, Vol. 140 (Materials Research Society, Pittsburgh, PA, 1989), pp. 215–226.
[20]J. M. Martin, C. Donnet, T. Le Mogne, and T. Epicier, Phys. Rev. B **48**, 10583 (1993); J. M. Martin, H. Pascal, C. Donnet, and T. Le Mogne, Surf. Coat. Technol. **68/69**, 427 (1994).
[21]Paper presented at the Society of Tribologists and Lubrication Engineers Conference, 17 May 1995, Chicago, IL (unpublished).
[22]*Handbook of X-ray Photoelectron Spectroscopy*, edited by C. D. Wagner, W. M. Riggs, L. E. Davis, J. F. Moulder, and G. E. Muilenberg (Perkin-Elmer, Eden Prairie, MN, 1979).
[23]*NIST X-ray Photoelectron Spectroscopy Database*, Version 1.0, edited by C. D. Wagner, written by D. M. Bickham (NIST, Gaithersburg, MD, 1989).
[24]C. Zhang, M. A. van Hove, and G. A. Somorjai, Surf. Sci. **149**, 326 (1985).
[25]N. Turner, J. S. Murday, and D. E. Ramaker, Analyt. Chem. **52**, 84 (1980).
[26]T. W. Haas, J. T. Grant, and G. J. Dooley, J. Appl. Phys. **43**, 1853 (1972).
[27]L. Muehlhoff, W. J. Choyke, M. J. Bozack, and J. T. Yates, Jr., J. Appl. Phy. **60**, 2842 (1986).
[28]K. S. Kim, W. E. Baitinger, J. W. Amy, and N. Winograd, J. Electron Spectrosc. Relat. Phenom. **5**, 351 (1974).
[29]T. A. Carlson, Surf. Interface Anal. **4**, 125 (1982).
[30]M. P. Seah and W. A. Dench, Surf. Interface Anal. **1**, 2 (1979).
[31]H. M. Kennett and A. E. Lee, Surf. Sci. **48**, 591, 606, 617, 624, 633 (1975).
[32]G. H. Smudde, Jr. and P. C. Stair, Surf. Sci. **317**, 65 (1994).

[33]J. M. Wilson, Surf. Sci. **53**, 315, 330 (1975); **57**, 499 (1976).
[34]L. J. Clarke, Surf. Sci. **102**, 331 (1981).
[35]M. Salmeron and G. A. Somorjai, Surf. Sci. **127**, 526 (1983).
[36]D. Jentz, S. Rizzi, A. Barbieri, D. Kelly, M. A. van Hove, and G. A. Somorjai, **329**, 14 (1995).
[37]J. M. Powers and G. A. Somorjai, Surf. Sci. **244**, 39 (1991).
[38]T. Le Mogne and I. L. Singer (unpublished data, 1993).
[39]G. Heinicke, *Tribochemistry* (Hanser, Munich, 1984).
[40]T. E. Fischer, Ann. Rev. Mater. Sci. **18**, 303 (1988).
[41]O. Kubaschewski and C. B. Alcock, *Metallurgical Thermochemistry*, 5th ed. (Pergamon, Oxford, 1979), Table A.
[42]Although it is possible to write and balance the equation $Mo+SO_2 \rightarrow MoS_2+MoO_3$ and show that the free energy of the products is lower than that of the reactants, Gibbs' phase rule disallows the reaction. The tie lines in Fig. 4 show why: In the reaction $MoO_2+SO_2 \leftrightarrow MoS_2+MoO_3$, the reactants are more stable than the products.
[43]A. D. Pelton, C. W. Bale, and W. T. Thompson, ''Equlibrium Product Calculation'' (version 21 February 1994) of the F*A*C*T system, Montreal, Quebecc, Canada, copyright 1986, thermfact LTD/LTEE. The program uses the well-known SOLGASMIX computational method.